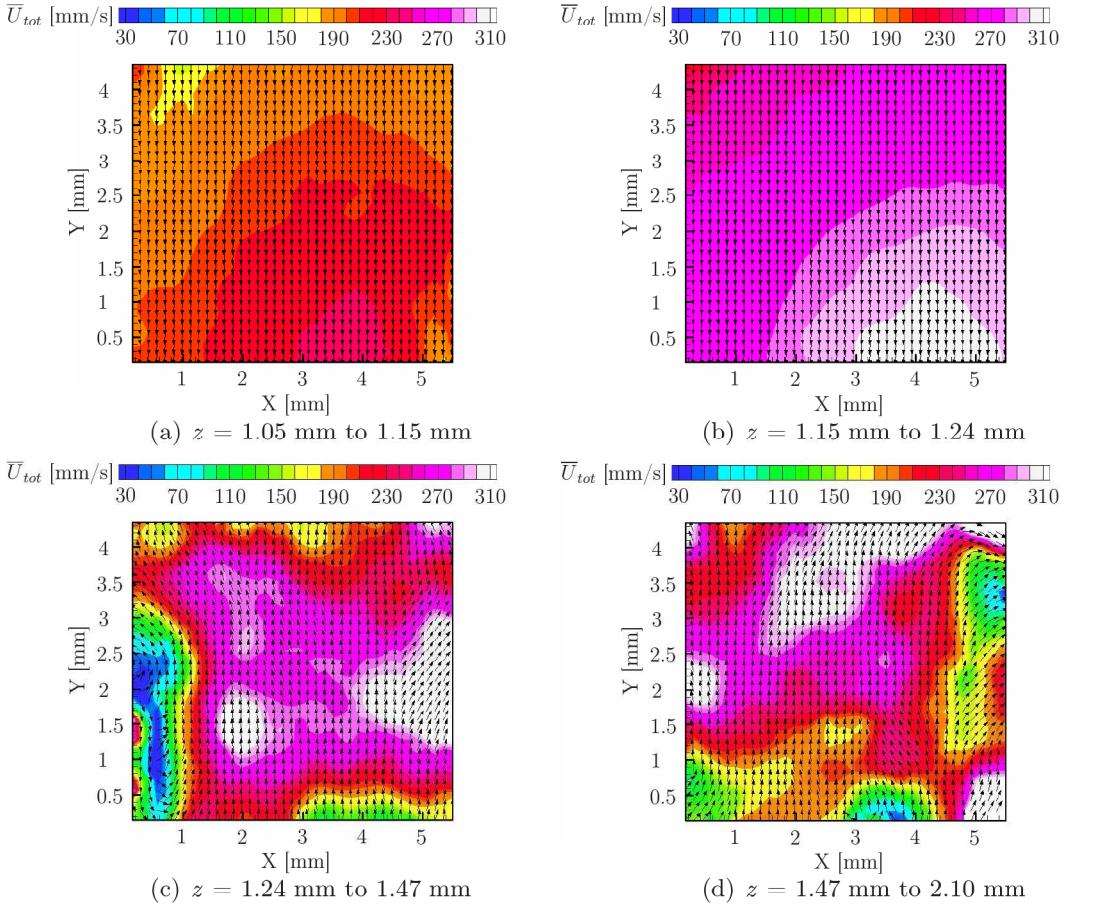

(a) z = 1.05 mm to 1.15 mm (b) z = 1.15 mm to 1.24 mm

(c) z = 1.24 mm to 1.47 mm (d) z = 1.47 mm to 2.10 mm

Figure 8.23: In-plane mean velocity distributions at different heights between z = 1.05 mm and 2.10 mm inside the laminar flow

Table 8.4: Experimental and theoretical mean velocity values for the different investigated layers inside the measurement volume

Physical depth in the film [mm]	**Measured mean velocity [mm/s]**	**Theoretical mean velocity [mm/s]**	**Numerical mean velocity [mm/s]**	**Deviation exp - theory [%]**
2.100	-	516.00	516.00	-
1.785	232.47 ± 9.11	438.50	438.65	47.0
1.355	232.39 ± 9.13	333.00	332.90	30.2
1.195	275.57 ± 2.12	294.00	293.60	6.3
1.100	204.88 ± 1.94	270.50	270.27	24.3
0.995	170.16 ± 2.32	244.50	244.49	30.4
0.805	136.25 ± 2.82	198.00	197.83	31.2
0.510	85.82 ± 3.08	125.50	125.36	31.6
0.175	39.14 ± 1.82	43.00	43.02	9.0
0	-	0	0	-

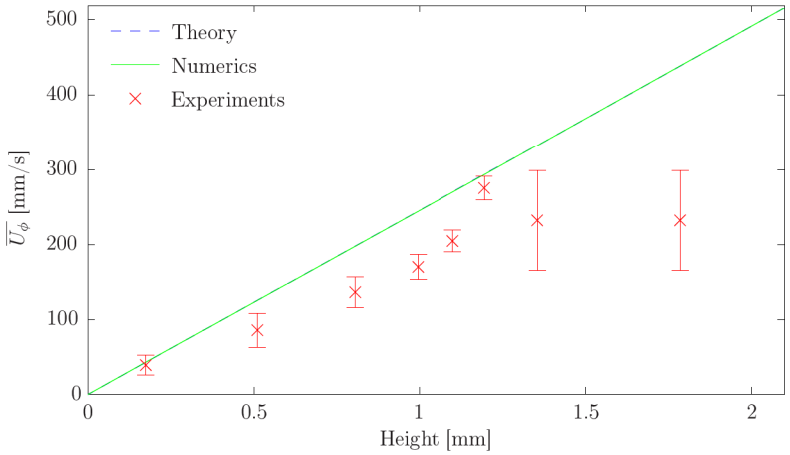

Figure 8.24: Comparison of measured in-plane mean velocity values with theoretical and numerical velocity distributions at different heights between $z = 0$ mm and 2.10 mm inside the laminar flow

at the two layers at mean depths of $z = 0.175$ mm and $z = 1.195$ mm.

The turbulence intensity fields for the different analyzed depths are shown in Figures 8.25 and 8.26 for, respectively, depths between $z = 0$ mm and 1.05 mm and between $z = 1.05$ mm and 2.10 mm. For most of the recorded flow field layers the turbulence intensity is below 20%, which is still quite high for a laminar flow, but can be explained by the rotating plexiglass disk, which rotated under a slight angle. This resulted in a vertical motion of $\pm$ 0.15 mm, which equals 14% of the total film depth. For both figures an area is found where high turbulence intensity levels are measured. These high turbulence levels can only be explained by large outliers in this area. The low laser intensity in the lower left corner of the recorded tracer particle images results in a wrong combination of tracer particle pairs during the inverse Fourier transformation, hence, in velocity outliers. To determine the mean velocity fields the average correlation method, described by Meinhart *et al.* [96], is used with which these calculated outliers are seen as noise and are therefore being canceled out. For the calculation of the turbulence intensity, however, the instantaneous cross correlation fields are used, thereby including the calculated outliers, which become visible by looking at the turbulence intensity distributions.

8.5 Summary

In this chapter, a new volumetric measurement technique has been presented in detail. This volumetric Particle Image Velocimetry technique is based on micro-PIV and makes use of a single digital camera and two optical monochromatic aberrations, namely astigmatism and the spherical lens aberration. In this way, the tracer particle positions in depth can be encoded by using a combination of these two monochromatic aberrations. With the use of this tracer particle depth-encoding the in-plane velocity fields at different layers in the investigated volume can be determined simultaneously, as well as the three-dimensional velocity fields, by making use of the particle-tracking method.

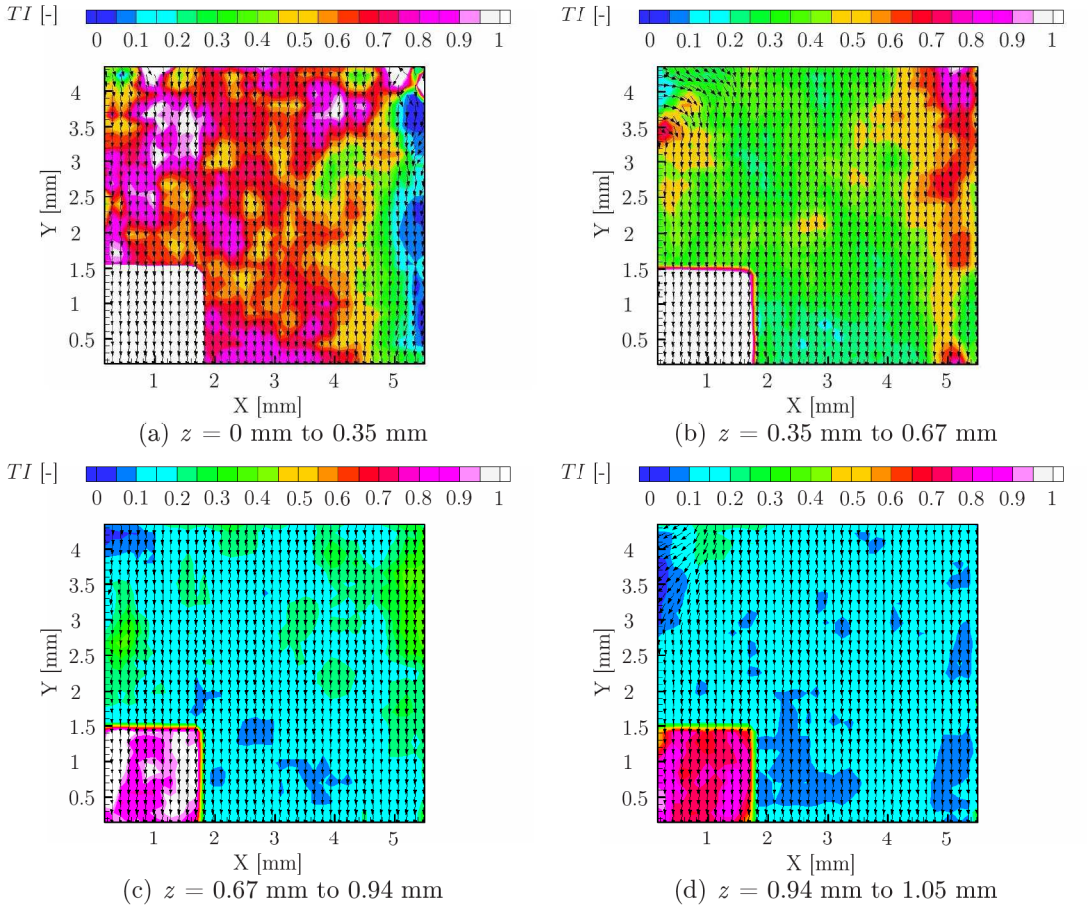

Figure 8.25: In-plane turbulence intensity distributions at different heights between $z = 0$ mm and 1.05 mm inside the laminar flow

The presentation of the measurement technique was split up into two main parts; the first part focussed on the image data processing algorithm, used to determine the velocity fields at different layers inside the investigated volume. The second part focussed on the mean velocity distributions and velocity fluctuations at different layers inside a thin laminar flow, used as a validation of the measurement technique.

The data processing algorithm consists of four main parts. The first part, the tracer particle image reconstruction algorithm, is used to recognise the tracer particle images at each recording and to determine their shapes and positions by making use of image intensity thresholds. After for all recordings the shapes and two-dimensional position of all tracer particles are found, each particle is assigned a three-dimensional position inside the investigated volume. This is done by making use of the central moments ratio of the tracer intensity distribution of each particle and comparing this value with the calibration curve. The tracer particle images are spread over many pixels due to the astigmatic imaging, which makes them unsuited for analysing the velocity. In order to decrease the size of a tracer particle image to an area of 9×9 pixels, the spherical blending technique of Angarita-Jaimes *et al* [2] is applied. The last step in the data processing algorithm focusses on obtaining the velocity fields at different slices inside the volume by applying particle discrimination.

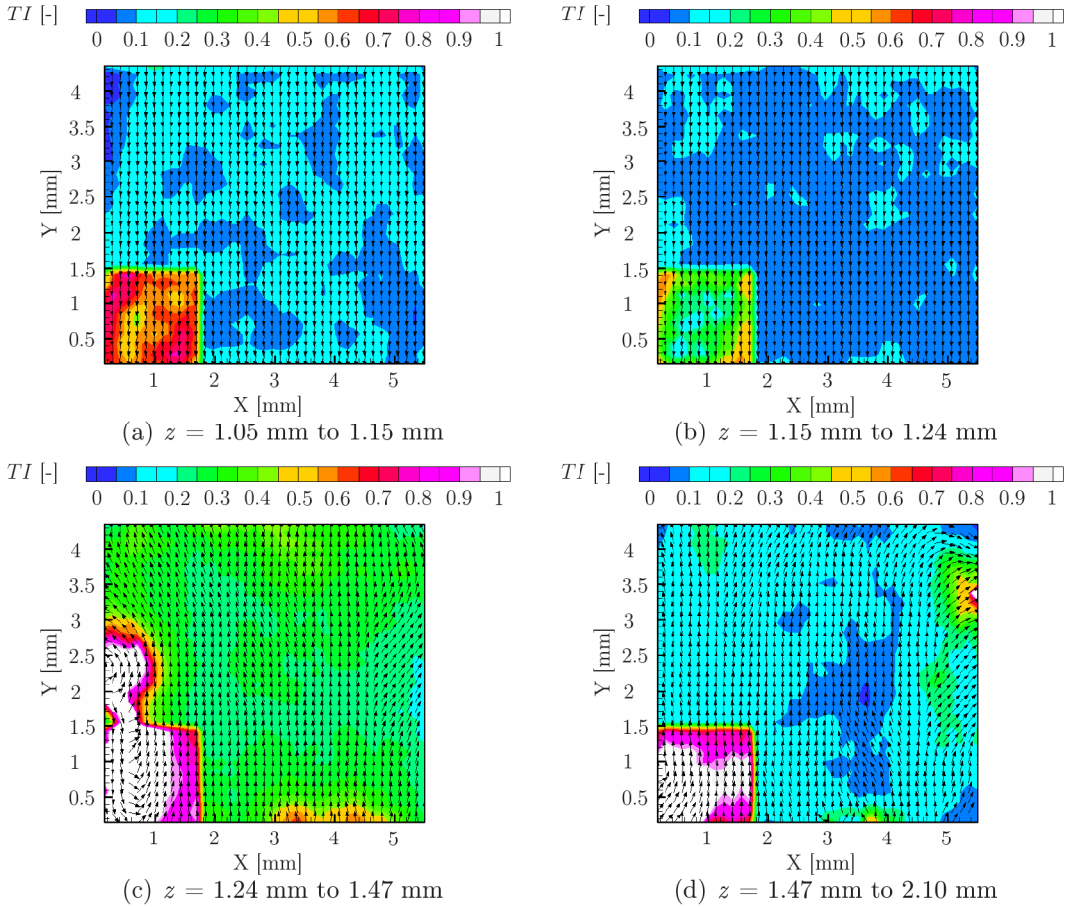

Figure 8.26: In-plane turbulence intensity distributions at different heights between $z = 1.05$ mm and 2.10 mm inside the laminar flow

This means, that only the particles at a certain depth are used to calculate the velocity fields, hereby discarding all other tracer particles.

To determine the mean velocity fields at a certain depth the average correlation method, described by Meinhart *et al.* [96], is used. With the use of two synthetically generated flows, i.e. a translational flow and a solid body rotational flow, this averaging method is validated. It has been shown that the results, obtained by using this method, are very satisfactory, hence, the average correlation method can be applied for analysing the measured flow fields.

To validate the volumetric measurement technique the three-dimensional flow field of a laminar flow is recorded. The obtained velocity fields at eight successive horizontal layers inside the recorded volume are compared with the theoretically calculated velocity values and the numerically simulated ones. It is observed that, although the directions of the flow fields at most investigated heights are correct and the values of the mean velocities are decreasing for increasing depth, the measured mean velocity values deviate quite much from the theory. This large difference is explained by the constant background intensity threshold over the whole image used for the image pre-processing. Due to the uneven distribution of the background noise over the recorded particle images, certain particles are given a higher central moments ratio, a lower depth determination of these particles; hence, resulting in a lower local particle displacement and flow velocity than the theoretical values.

Chapter 9

Conclusions and outlooks

Splashing of drops on liquid layers and spray impingement occurs in many industrial applications involving multi-phase flow of liquid drops in a gas, such as inside internal combustion engines with direct fuel injection and inside gas turbines, during spray drying, spray coating, spray cooling, etc. Investigations of the drop impingement onto liquid films have also importance in various agricultural and ecological fields, like the dispersion of anti-pesticides, the watering of plants, thereby assuring an equal distribution of the water drops, and the dispersion of seeds and microorganisms. It is encountered frequently in nature, leading to various phenomena such as the electrification of waterfalls, thunderstorm electrification and the formation of air bubbles during heavy rains, and can also be found in medical applications and forensic investigations. In all of these areas the impingement process of sprays plays a highly significant role. The impingement process itself, however, is until today not well understood and therefore still a very hot topic in fundamental research.

The present work has dealt with the single drop impingement processes upon steady and wavy liquid surface films of finite thickness, as well as the spray impingement onto rigid walls. The global aim of the present study was to develop a mathematical model of the single drop and spray impingement onto liquid films. To achieve this aim, the focus was put in particular on the description of the hydrodynamics of the wall surface film produced by spray impingement onto the wall, on a broader understanding of the physics involved in modeling of spray impingement processes and on the formulation of mathematical models based on experimental data and numerical simulations of the single drop impingement.

Two separate approaches were applied to obtain the necessary experimental and numerical results. The first approach focussed on the single drop impingement process upon steady and wavy liquid films of finite thickness, to understand in detail the physics behind the splash mechanism, the corona formation, the evolution of the cavity below the liquid surface and the typical time and length scales of the impingement process. With the use of these parameters mathematical models of the impingement process could be developed and implemented into the numerical codes for single drop and spray impingement. The second approach focussed on the direct measurement of the velocity distributions inside the wall film, produced by the impingement of a spray onto this rigid wall. A new measurement technique was developed to obtain the distributions of the mean and fluctuating film velocities under bad light conditions. By measuring the wall film velocity distributions under realistic conditions, not only the unsteady wall film flow, generated by the surrounding drop impingements, was taken into account, but also the interactions of drops with other impinging drops, both in the spray and during the interaction with the wall film.

In this study it was proven that with both methods reliable results could be obtained, which could be implemented into the already existing mathematical descriptions of the spray impingement process. In the following sections the useful and interesting observations have been summarised for both approaches.

Impingement of single drops onto steady liquid films of finite thickness

The analytical models, applied for the simulation of spray impingement processes, are mostly based on the experimental results of single drop impingements onto steady liquid films. In the best case, the experimental data of the inclined drop impingements are used. Sprays, however, are a collection of a large number of drops, where the outcome of each individual drop impingement onto a liquid film is influenced by the unsteady wall film flow, as well as by the interactions with other impinging drops, both in the spray and during the interaction with the wall film, all of them having a significant effect on the spray impingement process.

In order to show that not only the waviness of the liquid film, but also the velocity and amplitude of the surface film, has a significant influence on the spray impingement outcomes, measurements of the impingements of single drops onto steady liquid surface films of finite thickness and onto solitary surface waves were made. For the analysis of these results, emphasis was placed on the evolution of the cavity, appearing below the liquid surface upon impingement, in time, in particular on the time evolution of the depth of the cavity and the diameter of the cavity, measured at half its maximum depth.

For the initial phase of the impingement process onto steady liquid films a good correlation could be seen between the experimental data of the depth evolution of the cavity in time and the analytical approximation ($y^*_{cav} \sim t^{*2/5}$). For the same non-dimensional time instants it was observed that the time evolution of the diameter correlated well with the remote asymptotic solution, derived by Yarin and Weiss [196] for single drop impingements onto deep pools ($D^{*2}_{cr} \sim t^*$). For larger non-dimensional times a deviation was found between the experiments and the theory for both length scales. For the depth evolution, this deviation resulted from the vicinity of the cavity tip to the bottom of the film, and increased faster for lower values of the initial surface film thickness. The deviation between the experiments and theory for the time evolution of the diameter was caused by the fact that the theoretical description did not account for the influence of the surface tension, gravity and the interaction of the expanding cavity with the bottom of the liquid film.

Concerning the overall impingement process it was found that the velocity with which the cavity penetrated into the liquid film was constant, $U^*_{cav} = 0.5$, and independent of the initial film thickness, Weber number of the impinging drop and liquid properties. The time at which the cavity reached its maximum depth depended on the initial liquid film thickness, being larger for larger initial film thicknesses, although this behaviour was not linear, due to the larger expanded cavity and subsequent higher surface tension forces for thicker surface films. The time at which the cavity started its retraction phase was independent of the surface film thickness, but correlated linearly with the Weber number of the impinging drop and the surface tension of the liquid. A higher Weber number led to a later retraction of the cavity, since surface tension forces could be overcome for a longer time by inertia. The same behaviour was found for a lower value of the surface tension, where the surface tension forces, responsible for the retraction of the cavity, were lower.

The impingement upon a thicker surface film resulted in a lower expansion of the cavity,

due to the larger surface tension forces and the effect of gravity that had to be overcome. The same effect was seen for lower Weber numbers of the impinging drops, hence less available inertia to overcome the surface tension forces, and for liquids with higher surface tensions, due to which the surface tension forces, opposing the expansion of the cavity, were higher. The non-dimensional time instant at which the maximum diameter of the cavity was reached, was independent of the initial thickness of the liquid surface film, but depended linearly on the Weber number of the impinging drop and on the surface tension of the liquid. For a higher value of the Weber number and for a lower value of the surface tension, the maximum diameter was reached later, since inertia could overcome the surface tension forces easier and for a longer time. The corresponding value of the maximum diameter of the cavity was subsequently larger for higher Weber numbers and lower values of the surface tension. The decrease of the cavity diameter during the receding phase of the impingement process was not influenced by the thickness of the initial surface film. A lower value of the surface tension of the liquid, however, led to a longer period during which the receding took place, whereas a lower Weber number resulted in a faster receding and retraction of the cavity. The analytical models, based on the propagation of a kinematic discontinuity (Yarin and Weiss [196]) and describing the time evolution of the cavity diameter, the maximum cavity diameter and the time this maximum cavity diameter was reached, predicted the experimental data very accurately.

With the use of the results of the numerical simulations the time evolution of the residual film thickness was analysed. The minimum residual film thickness was found to relate directly to the Reynolds number of the impinging drop and could be described by $h^*_{res} \sim Re^{-2/5}$. For very high Reynolds numbers the asymptotic value of the minimum residual film thickness increased for increasing thickness of the initial surface film.

Concerning the numerical simulations it has been shown that the differences between the axi-symmetrical simulations and the fully three-dimensional simulations were only minor and focussed mainly on the receding phase of the cavity. Due to the three-dimensional simulation of the impingement process, the flow of the rim was solved in a three-dimensional way, resulting in a lower curvature of the capillary wave during the receding phase. This led to a lower pressure difference between the leading and the trailing edge of the capillary wave and thus a lower vertical wave velocity. The subsequent receding of the cavity took longer and the retraction of the cavity was later, which led to a better correlation between the experimental data and the numerical simulations.

Single drop impingement onto wavy liquid films

The analytical models, based on the experimental data obtained for single drop impingements upon steady liquid surface films, are commonly used for the modeling of spray impingement processes, by applying the superposition principle. This means that the impingement of each drop inside the spray is modeled individually, by assuming that no other drops are present within a certain boundary around the impingement area, hence the impingement of each single drop of the spray is not influenced by other surrounding drop impingements. Sprays, however, are a collection of a large number of drops, where the outcome of each individual drop impingement onto a liquid film is influenced by the unsteady wall film flow, generated by the surrounding impingements, as well as by the interactions with other impinging drops, both in the spray and during the interaction with the wall film. All of these factors have a significant effect on the spray impingement process, thereby drastically changing the mathematical

description of the spray impingement. In this work it has been shown that the impingement process is highly influenced by the topology of the liquid surface film. The impingement upon two different classes of surface waves, the standing waves and the solitary surface waves, have been investigated. For the first class of waves the influence of the inclination of the surface on the impingement outcomes was studied, whereas for the solitary surface waves also the velocity distribution inside the liquid film was taken into account, which is a significant parameter for spray impingement.

For the impingement process upon standing waves, it was found that the penetration of the cavity in depth direction was independent of the inclination angle of the liquid surface and the Weber number, whereas a clear influence of the inclination was observed for the radial expansion. Because of the declining surface film and the constant penetration of the cavity in depth, a larger surface of the cavity was present at the left side of the cavity, resulting in larger values of the surface tension forces and therefore a faster conversion of the kinetic energy. Although the time evolution of the total diameter of the cavity was not influenced by the inclination angle, the inclination of the standing wave led to lower values of the cavity diameter at the left side of the cavity. This difference between the diameters of the cavity at both sides increased more for lower Weber numbers.

Due to the lower rim at the left side of the cavity and the subsequent earlier merging of the rim with the liquid surface, the capillary wave was formed earlier at this side, thereby introducing several clear differences between the cavities formed after impingement upon steady liquid films and standing waves: a lower value of the maximum diameter of the cavity, an asymmetrical downward motion of the capillary waves and receding of the cavity, leading to large differences between the values of the local diameters at both sides of the cavity, an asymmetrical merging of the capillary waves and an off-axis Worthington jet of which its inclination and curvature increased with increasing Weber number.

The propagation of the liquid surface film, as was the case for the solitary surface wave, had a distinct influence on the outcome of the impingement process and on the time evolution of the cavity shape. The solitary wave induced a relative velocity component onto impingement, due to which the shape and inclination of the corona were changed. Additionally, as a result of the decreasing horizontal velocity component inside the liquid film with increasing depth, the cavity inclined in the direction of the wave propagation, resulting in an asymmetrical expansion of the cavity during the first stages after impingement. The presence or absence of the capillary waves at the left and/or right side of the cavity, in combination with the unequal distribution of the surface tension forces over the cavity surface induced an asymmetrical receding and retraction of the cavity, as well as an inclined Worthington jet.

By varying the phase of the solitary surface wave at impingement between $0° \leq \varphi \leq 180°$, a clear difference in the prompt splash mechanism and the formation of the corona was present. Depending on the wave-phase strong interactions of the expanding corona with the leading or trailing edge of the solitary wave were the result. For relatively low phase angles large cavities with a sharp inclination in the direction of the wave propagation were formed, whereas for relatively high phases the expansion phase of the cavity was influenced only in a minor way. The formation, strength and movement of the capillary waves changed magnificently for different phases. For small phases a single strong capillary wave was formed at the left side of the cavity, for intermediate phases at the right side and for large phases at both sides of the cavity, but lagged in time between the left and right side of the cavity. These differences led to completely

different recedings and retractions of the cavities and subsequent different Worthington jets.

Concerning the typical length and time scales of the drop impingement process, it was found that for the small amplified surface wave the maximum depths and absolute diameters of the cavities, as well as the non-dimensional time instants at which these length scales were reached, were constant and independent of the phases of the wave at impingement and the liquid properties. For the values of the maximum absolute diameter, a weak dependency on the viscosity of the liquids was found, where it was observed that a higher viscosity resulted in a slightly higher value of the absolute maximum depth. For the large amplified wave the values of the maximum depths and absolute diameters of the cavities showed no dependency on the phases of the wave at impingement and the liquid properties, whereas for the values of the non-dimensional time instants a linear increase with increasing wave-phases was observed. The dependency of the values of the maximum absolute diameter on the viscosity of the liquids, found for the impingement upon small solitary waves, had disappeared for the large amplified wave.

A higher Weber number of the impinging drop led to a pronounced prompt splash, a higher, larger and unstable corona and a cavity with a larger maximum diameter and depth. An inclination of the cavity was observed for all Weber numbers, where the angle of inclination increased sharply for larger Weber numbers. For lower Weber numbers an earlier receding and retraction occurred; the receding itself, however, was for all Weber numbers highly asymmetrical, due to the presence of a strong capillary wave at the right side and the absence or presence of a weak capillary wave at the left side of the cavity.

For the small amplified wave both typical length scales showed a linear increasing behaviour with the mean Weber number. The time at which the maximum depth was reached increased quadratically with an increase of the mean Weber number, whereas an increasing linear behaviour was found between the mean Weber number and the time of maximum absolute diameter. For these typical length and time scales it was found that for the same Weber number the values were larger for the liquid with the higher viscosity, due to the lower maximum amplitude and velocity of the surface wave. For the large amplified wave larger values of the maximum depths, but approximately constant values of the maximum absolute diameter, were found. The time at which the maximum depth was reached, increased quadratically with an increase of the mean Weber number, whereas a linear behaviour was found between the mean Weber number and the time of maximum absolute diameter. The values of both length and time scales did not depend on the liquid properties, meaning that for large amplified waves, hence with a large propagation velocity and maximum amplitude, the viscosity did not play a role anymore in the impingement process.

A comparison of the results between both solitary surface waves led to the conclusion that due to the higher propagation velocity and higher amplitude of the larger surface wave a very significant difference between the relative diameters of both sides of the cavity occurred, together with a stronger interaction of the expanding rim with the leading or trailing edge of the surface wave. This led to a cavity, having a smaller maximum depth and absolute diameter, although the typical time scales remained approximately the same.

Direct measurement of film velocity at spray impingement

Sprays are a collection of a large number of drops, where the outcome of each individual drop impingement onto a liquid film is influenced by the unsteady wall film flow and by the

interactions with other impinging drops. In order to mathematically describe the spray impingement process, it is necessary to be able to predict the three-dimensional distributions of the velocity inside the liquid wall film. Because of the highly fluctuating character of this wall film and the presence of many small and large droplets close to this film, most of the standard measurement techniques are not adequate enough. To overcome these problems, a new volumetric measurement technique has been presented in this thesis. This volumetric Particle Image Velocimetry technique is based on micro-PIV and makes use of a single digital camera and two optical monochromatic aberrations, namely astigmatism and the spherical lens aberration. In this way, the tracer particle positions in depth can be encoded by using a combination of these two monochromatic aberrations. With the use of this tracer particle depth-encoding the in-plane velocity fields at different layers in the investigated volume can be determined simultaneously, as well as the three-dimensional velocity fields, by making use of the particle-tracking method.

The validation of this measurement technique, with the use of a laminar flow, showed that, although the directions of the flow fields at most investigated heights were correct and the values of the mean velocities were decreasing for increasing depth, the measured mean velocity values deviated quite much from the theory. This large difference was the result of the constant background intensity threshold setting over the whole image, which was, however, incorrect due to the uneven distribution of the background noise over the recorded particle images. This resulted in certain particles that were given a higher central moments ratio, resulting in a lower depth determination of these particles and therefore a lower local particle displacement and flow velocity than the theoretical values.

With the use of this measurement technique the radial mean velocities of the wall film and their fluctuations have been investigated under the variation of different impinging parameters of the sprays, produced by ultrasonic nozzles. It was found that the swirling motion of the spray came clearly forward in the large vortices present in the surface films at both investigated impingement heights for both nozzles. The centers of these large vortices corresponded to the centers of the impinging sprays. The carrier gas changed the swirl direction of the spray in such a way that sprays, obtained for both nozzles using the carrier gas, as well as the corresponding vortices inside the surface films were rotating in clockwise direction for both impingement heights, whereas the surface film vortices for impinging sprays without carrier gas were rotating in an anticlockwise sense.

For increasing impingement heights a clear decrease of the mean radial film velocities was found, as a result of the decrease of the mean vertical velocity of the sprays and the subsequent decrease of the kinetic energy. This resulted in a decrease of the radial film velocities induced by the cavities, appearing in the surface film at drop impingement.

For larger volume flows the areas with relatively high mean radial film velocities, as well as the values of the maximum absolute radial film velocities, were increasing, because an increase in volume flow was directly linked to an increase in the kinetic energy of the drops of the spray. However, no clear dependency of an increase in volume flow on the surface film mean radial velocity directions was found, nor a dependency of the impingement height on the directions of the streamlines or on the size and strength of the surface film vortices.

At radial positions of the surface film, where relatively high mean radial film velocities were observed, low values of the velocity fluctuations were found. Regions in the surface film, where the flow was mainly in one of both directions, the velocity fluctuations in this particular direction were higher, whereas at the positions of saddle points and vortex cores the fluctuations in both directions were strong.

Suggestions for future research on single drop and spray impingement

Attention should be paid for further improvement of the experimental and numerical library of the single drop and spray impingement outcomes, as well as in the modeling of single drop impingements onto traveling surface waves and the velocity distributions inside the wall film during spray impingement.

Before we proceed with the recommendations for future work, the important role of the measurements of single drops impingements onto traveling surface waves in spray modeling and validation has to be emphasised. Sprays are a collection of a large number of drops, where the outcome of each individual drop impingement onto a liquid film is influenced by the unsteady wall film flow, generated by the surrounding impingements, as well as by the interactions with other impinging drops, both in the spray and during the interaction with the wall film. All of these factors have a significant effect on the spray impingement process, thereby drastically changing the mathematical description of the spray impingement. However, before one can model spray impingement in detail, the physics behind the impingement of single drops onto wavy liquid films has to understood. In this thesis it has been shown that the waviness, hence inclination, of the surface film, as well as the velocity and amplitude of the surface waves, have a highly significant influence on the single drop impingement results, in particular on the splash mechanism, the corona formation, the evolution of the cavity below the liquid surface and the typical time and length scales of the impingement process. This means that the existing theoretical models, used for the modeling of spray impingement, should definitely be changed by taking into account the significant influences of the film topology on the impingement processes.

The topology of the liquid film, used for the numerical simulations of the impingements of single drops onto a wavy liquid surface, has been set to the standing wave without continuous added energy. This means that at the start of the simulation a surface wave is initiated, which levels off in time due to the influence of surface tension and gravity into a steady liquid film of thickness h. The use of this special standing wave can be justified by the fact that this leveling process takes much longer than the drop impingement process itself, due to which the wavy liquid surface still influences the cavity below the liquid surface at the end of the impingement process. Physically, however, two important factors have to be taken into account. First of all, the waves present at the surface of the wall film for spray impingement, are no standing waves, but traveling waves. This means that also the distribution of the film velocity plays a significant role in the impingement process, as has been shown in this thesis with the use of experimental data. Second, the continuous impingement of drops of the spray assure a continuous local supply of kinetic energy to the liquid film, due to which no leveling of the surface film will take place during the impingement process. These two factors should be taken into account for future simulations, because the experimental data can then be used as a direct validation of the obtained numerical results.

The presented experimental results of the single drop impingement process upon solitary surface waves have focussed onto the differences between two liquids, namely distilled water and a glycerine/water mixture with 30 Vol% glycerine. The influence of the viscosity on the cavity evolution in time could therefore be shown for the small amplified waves, whereas for the large amplified waves it was shown that the viscosity of the liquid does not play a role anymore. The dependency of the typical length and time scales on the Weber number could only be proven by the difference in terminal velocity of the impinging drop, because the surface

tension of both liquids was in the same order of magnitude. It is therefore necessary to conduct more impingement measurements with liquids having various surface tensions, to obtain a clear relation between the time and length scales and the Weber number.

To simulate the topology of the wall surface film during spray impingement, a solitary surface wave with various amplifications has been generated into a deep pool. The question, however, rises to what extent these film topologies coincide. Further experimental research has to be conducted, where also the single drop impingement onto continuously traveling surface waves has to be taken into account. In this way, the fluctuations in the propagation direction of the wave on the impingement process can be studied in more detail. Impinging sprays usually generate a surface film with a thickness that is in the same order of magnitude as the drop diameter. To investigate the influence of the bottom of the liquid film on the cavity evolution in time for the impingement onto a wavy liquid film, the thickness of the surface film has to be varied.

The velocity fluctuations inside the wall film for spray impingement are highly three-dimensional. In order to obtain a qualitatively high reliable model for the wall film hydrodynamics, it is necessary to measure simultaneously these three-dimensional velocity distributions inside the liquid film. Furthermore, to link these three-dimensional velocity distributions to the velocity and diameter distributions of the spray before impingement, three-dimensional phase-Doppler measurements need to be done.

The validation measurements of the presented measurement technique show a relatively large deviation of the measured mean velocity values from the theory. This large difference is the result of the constant background intensity threshold over the whole image. Due to the uneven distribution of the background noise over the recorded particle images, certain particles are given a higher central moments ratio, resulting in a lower depth determination of these particles; hence, resulting in a lower local particle displacement and flow velocity than the theoretical values. This problem can be overcome by assigning to each tracer particle in the recordings its own local background threshold by optimizing its background intensity level, which still has to be implemented into the image processing code.

Bibliography

[1] Albrecht, H.E., Borys, M., Damaschke, N., Tropea, C. (2003) *Laser Doppler and phase Doppler measurement techniques*. Springer-Verlag Berlin Heidelberg New York, 2003

[2] Angarita-Jaimes, N., McGhee, E., Chennaoui, M., Campbell, H.I., Zhang, S., Towers, C.E., Greenaway, A.H., Towers, D.P. (2006) *Wavefront sensing for single view three-component three-dimensional flow velocimetry*. Exp. Fluids, **41**, 881 - 891

[3] Angele, K.P., Suzuki, Y., Miwa, J., Kasagi, N., Yamaguchi, Y. (2005) *Development of a high-speed scanning micro-PIV system*. Proc. 6^{th} Int. Symp. Particle image Velocimetry, Pasadena, USA

[4] Bai, C., Gosman, A.D. (1995) *Development of methodology for spray impingement simulation*. SAE 950283

[5] Bai, C., Gosman, A.D. (1996) *Mathematical modeling of wall films formed by impinging sprays*. SAE 960626

[6] Bai, C., Rusche, H., Gosman, A.D. (2002) *Modeling of gasoline spray impingement*. Atom. Sprays, **12**, 1 - 27

[7] Bakshi, S., Roisman, I.V., Tropea, C. (2007) *Investigations on the impact of a drop onto a small spherical target*. Phys. Fluids, **19**, 032102-1 - 032102-12

[8] Barnes, H.A., Hardalupas, Y., Taylor, A.M.K.P., Wilkins, J.H. (1999) *An investigation of interaction between two adjacent impinging droplets*. Proc. 15^{th} Ann. Conf. Liquid Atom. Spray Systems, Toulouse, France

[9] Barnhart, D.H., Adrian, R.J., Papen, G.C. (1994) *Phase-conjugate holographic system for high-resolution particle image velocimetry*. Appl. Opt., **30**, 7159 - 7170

[10] Beberovic, E., van Hinsberg, N.P., Jakirlic, S., Roisman, I.V., Tropea, C. (2009) *Drop impact onto a liquid layer of finite thickness: Dynamics of the cavity evolution*. Phys. Rev. E, **79**, 036306-1 - 036306-15

[11] Bergmann, R., Meer, D., van der, Stijnman, M., Sandtke M., Prosperetti, A., Lohse, D. (2006) *Giant bubble pinch-off*. Phys. Rev. Letters, **96**, 154505-1 - 4

[12] Birkhoff, G., MacDougall, D.P., Pugh, E.M., Taylor, G. (1948) *Explosives with lined cavities*. J. Appl. Physics, **19**, 563 - 582.

[13] Blondel, D., Roisman, I.V., Tropea, C., Wenzel, S. (2001) *Investigation of impinging diesel spray applying optical methods of measurements*. Proc. 17^{th} Ann. Conf. Liquid Atom. Spray Systems, Zürich, Switserland

[14] Böhm, C.A. (2002) *Wechselwirkung von Tropfen und Sprays newtonischer und nichtnewtonischer Fluide mit festen Oberflächen: Aufprall und Filmbildung*. Ph.D. Thesie, Technische Universität Darmstadt, Germany

[15] Böhm, C.A., Weiss, D.A., Tropea, C. (1999) *Multi-droplet impact onto solid walls: droplet-droplet interaction and collision of kinematic discontinuities*. Proc. 16^{th} Ann. Conf. Liquid Atom. Spray Systems, Darmstadt, Germany

[16] Bown, M.R., Macinnes, J.M., Allen, R.W.K., Zimmerman, W.B.J. (2005) *Three-component microfluidic velocity measurements using stereoscopic Micro-PIV*. Proc. 6^{th} Int. Conf. Liquid Atom. Spray Systems, Pasadena, USA

[17] Brackbill, J.U., Kothe, D.B., Zembach, C. (1992) *A continuum method for modeling of surface tension*. Comp. Phys., **100**, 335 - 354

[18] Brenn, G., Valkovska, D., Danov, K.D. (2001) *The formation of satellite droplets by unstable binary drop collisions*. Phys. Fluids, **13**, 2463 - 2477

[19] Brücker, C. (1995) *Digital-Particle-Image-Velocimetry (DPIV) in a scanning light-sheet: 3D starting flow around a short cylinder*. Exp. Fluids, **19**, 255 - 263

[20] Brücker, C. (1996) *3-D Scanning-particle-image-velocimetry: technique and application to a spherical cap wake flow*. Appl. Sci. Res., **56**, 157 - 179

[21] Brunton, J.H. (1966) *High speed liquid impact*. Proc. R. Soc. London - A, **260**, 79 - 85

[22] Chiu, W.C., Rib, L.N. (1956) *The rate of dissipation of energy and the energy spectrum in a low-speed turbulent jet*. Trans. Am. Geophys. Union, **37**, 13 - 26

[23] Coghe, A., Cossali, G.E., Marengo, M. (1995) *A first study about single drop impingement on thin liquid film in a low Laplace number range*. Proc. PARTEC'95, Nürnberg, Germany

[24] Cossali, G.E., Coghe, A., Marengo, M. (1997) *The impact of a single drop on a wetted solid surface*. Exp. Fluids, **22**, 463 - 472

[25] Cossali, G.E., Marengo, M., Santini, M. (2004) *Impact of single and multiple drop array on liquid film*. Proc. 19^{th} Ann. Conf. Liquid Atom. Spray Systems, Nottigham, UK

[26] Cossali, G.E., Marengo, M., Coghe, A., Zhdanov, S. (2004) *The role of time in single drop splash on thin film*. Exp. Fluids, **36**, 888 - 900

[27] Cresswell, R.W., Morton, B.R. (1995) *Drop-formed vortex rings - The generation of vorticity*. Phys. Fluids, **7**, 1363 - 1370

[28] Dear, J.P., Field, J.E. (1987) *High-speed photography of surface geometry effect in liquid/solid impact*. J. Appl. Physics, **63**, 1015 - 1021

[29] Desantes, J.M., Arrègle, J., Pastor, J.V. (1998) *Diesel spray wall impingement characterisation by means of P.D.A. and high speed visualisation*. Proc. 9^{th} Int. Symp. Appl. Laser Tech. Fluid Mech., Lisbon, Portugal

[30] Ebara, T., Amagai, K., Arai, M. (1997) *Movement and structure of diesel spray impinging on an inclined wall*. SAE 970046

[31] Eggers, J., Fontelos, M.A., Leppinen, D., Snoeijer, J.H. (2007) *Theory of the colapsing axisymmetric cavity.* Phys. Rev. Letters, **98**, 094502-1 - 4

[32] Elmore, P.A., Chahine, G.L., Oğuz, H.N. (2001) *Cavity and flow measurements of reproducible bubble entraimnent following drop impacts.* Exp. Fluids, **31**, 664 - 673

[33] Elsinga, G.E., Scarano, F., Wieneke, B., Van Oudheusden, B.W. (2005) *Tomographic particle image velocimetry.* Proc. 6^{th} Int. Conf. Liquid Atom. Spray Systems, Pasadena, USA

[34] Elsinga, G.E., Scarano, F., Wieneke, B., Van Oudheusden, B.W. (2006) *Tomographic particle image velocimetry.* Exp. Fluids, **41**, 933 - 947

[35] Elsinga, G.E., Wieneke, B., Scarano, F., Schröder, A. (2008) *Tomographic 3D-PIV and applications.* Particle Image Velocimetry, Springer, Germany

[36] Elsinga, G.E., Wieneke, B., Scarano, F., Van Oudheusden, B.W. (2005) *Assessment of Tomo-PIV for three-dimensional flows.* Proc. 6^{th} Int. Conf. Liquid Atom. Spray Systems, Pasadena, USA

[37] Engel, O.G. (1966) *Crater depth in fluid impacts.* J. Appl. Physics, **37**, 1798 - 1808

[38] Engel, O.G. (1967) *Initial pressure, initial flow velocity, and the time dependence of crater depth in fluid impacts.* J. Appl. Physics, **38**, 3935 - 3940

[39] Eres, M.H., Schwartz, L.W. (2001) *Spraying and spreading processes on moving substrates.* Proc. 4^{th} Europ. coating Symp., Brussels, Belgium

[40] Estrade, J.-P., Carentz, H., Lavergne, G., Biscos, Y. (1999) *Experimental investigation of dynamic binary collision of ethanol droplets - a model for droplet coalescence and bouncing.* Int. J. Heat Fluid Flow, **20**, 486 - 491

[41] Fabry, E.P., Sieverding, C.H. (2000) *3D stereoscopic holographic PIV in swirling flows and turbomachine cascades.* Particle Image Velocimetry: Progress towards Industrial Application, Kluwer Academic Publishers, 2000

[42] Fedorchenko, A.I., Wang, A.-B. (2004) *On some common feature of drop impact on liquid surfaces.* Phys. Fluids, **16**, 1349 - 1365

[43] Fischer, R.E., Tadic-Galeb, B. (2000) *Optical system design.* McGraw-Hill, 2000

[44] Fromm, A. (2009) *Numerical simulation of drop impact onto a stationary/oscillating liquid layer of finite thickness.* Master Thesis, Technische Universität Darmstadt, Germany

[45] Fujimoto, H., Senda, J., Nagae, M., Hashimoto, A. (1990) *Characteristics of a diesel spray impinging on a flat wall.* Proc. Int. Symp. COMODIA 90, Kyoto, Japan

[46] Fukai, J., Shiiba, Y., Yamamoto, T., Miyatake O., Pouilikakos, D., Megaridis, C.M., Zhao, Z. (1995) *Wetting effects on the spreading of a liquid droplet with a flat surface: Experiment and modeling.* Phys. Fluids, **7**, 236 - 247

[47] Garcia-Sucerquia, J., Xu, W., Jericho, S.K., Klages, P., Jericho, M.H., Kreuzer, H.J. (2006) *Digital in-line holographic microscopy.* Appl. Opt., **45**, 836 - 850

[48] Gauthier, V., Riethmuller, M.L. (1988) *Application of PIDV to complex flows: Measurements of third component*. Von Karman Institute Lecture Series, **6**

[49] Georjon, T.L., Reitz, R.D. (1999) *A drop-shattering collision model for multidimensional spray computations*. Atom. Sprays, **9**, 231 - 254

[50] Gharib, M., Pereira, F., Castaño Graff, E. (2003) *Defocusing 3-D PIV technique and its performance with respect to stereographic systems*. Proc. 5^{th} Int. Symp. Particle image Velocimetry, Busan, Korea

[51] Griebel, P. (1997) *Untersuchung zur scahdstoffarmen, atmosphärischen Verbrennung in einem Fett-Mager-Brennkammersektro für Flugtriebwerke*. Ph.D. Thesis, Deutsches Zentrum für Luft- und Raumfahrt e.V., Germany

[52] Hadamard, J.S. (1911) *Slow permanent motion of a viscous liquid sphere in a viscous fluid*. C.R. Acad. Sci., **152**, 1735 - 1738

[53] Hain, R., Kähler, C.J. (2006) *3D3C time-resolved measurements with a single camera using optical abberations*. Proc. 13^{th} Int. Symp. Appl. Laser Tech. Fluid Mech., Lisbon, Portugal

[54] Hall, D.D., Mudawar, I. (1995) *Experimental and Numerical study of quenching complex-shaped metallic alloys with multiple, overlapping sprays*. Int. J. Heat Mass Transfer, **38**, 1201 - 1216

[55] Han, Z., Xu, Z., Trigui, N. (2000) *Spray/wall interaction models for multidimensional engine simulation*. Int. J. Engine Research, **1**, 127 - 146

[56] Harlow, H., Shannon, J.P. (1967) *The splash of a liquid drop*. J. Appl. Phys., **38**, 3855 - 3866

[57] Hinsch, K.D. (1993) *The many dimensions of optical flow diagnostics*. SPIE, **2052**, 63 - 78

[58] Hinsch, K.D. (2002) *Holographic particle image velocimetry*. Meas. Sci. Technol., **13**, R61 - R72

[59] Hirt, C., Nichols B. (1981) *Volume of Fluid (VOF) Method for the dynamics of free boundaries*. J. Comp. Physics, **39**, 201

[60] Hobbs, P.V., Osheroff, T. (1967) *Splashing of drops on shallow liquids*. Science, **158**, 1184 - 1186

[61] Hori, T., Sakakibara, J. (2004) *High-speed scanning stereoscopic PIV for 3D vorticity measurements in liquids*. Meas. Sci. Technol., **15**, 1067 - 1078

[62] Ishiguro, R., Rolley, E., Balibar, S., Eggers, J. *The dripping of a crystal*. Internet: http://www.lps.ens.fr/ balibar/dripping.pdf

[63] Issa, R.I. (1986) *Solution of the implicity discretised fluid flow equations by operator-splitting*. J. Comp. Physics, **62**, 40 - 65

[64] Jasak, H., Weller, H.G., Gosman, A.D. (1999) *High resolution NVD differencing scheme for arbitrary unstructured meshes*. Int. J. Num. Methods Fluids, **31**, 431 - 449

[65] Jayarantne, D.W., Mason, B.J. (1964) *The coalescence and bouncing of water drops at an air/water interface.* Proc. R. Soc. London - A, **280**, 545 - 565

[66] Jong-Leng, L. (2001) *Splash formation by spherical drops.* J. Fluid Mech., **427**, 73 - 105

[67] Kähler, C.J., Kompenhans, J. (2000) *Fundamentals of multiple plane stereo particle image velocimetry.* Exp. Fluids, **29**, S70 - S77

[68] Kalantari, D., Tropea, C. (2006) *Spray impact onto flat and rigid walls: Emperical characterization and modelling.* Int. J. Multiphase Flow, **33**, 525 - 544

[69] Kalantari, D., Tropea, C. (2007) *Phase Doppler measurements of spray impact onto rigid walls.* Exp. Fluids, **43**, 285 - 296

[70] Katsura, N., Saito, M., Senda, J., Fujimoto, H. (1989) *Characteristics of a diesel spary impinging on a flat wall.* SAE 890264

[71] Ko, K., Arai, M. (2002) *Diesel spray impinging on a flat wall, part I: characteristics of adhered fuel film in an impingement diesel spray.* Atom. Sprays, **12** 737 - 751

[72] Ko, K., Arai, M. (2002) *Diesel spray impinging on a flat wall, part II: volume and average air-fuel ratio of an impingement diesel spray.* Atom. Sprays, **12** 753 - 768

[73] Ko, G.H., Lee, S.H., Ryou, H.S., Chio, Y.K. (2003) *Development and assessment of a hybrid droplet collision model for two impinging sprays.* Atom. Sprays, **13**, 251 - 272

[74] Ko, G.H., Ryou, H.S. (2005) *Modeling of droplet collision-induced breakup process.* Int. J. Multiphase Flow, **31**, 723 - 738

[75] Lecerf, A., Trinité (2000) *Stereoscopic PIV: Translation method.* Particle Image Velocimetry: Progress towards Industrial Application, Kluwer Academic Publishers, 2000

[76] Lee, J., Bergman, T. (2001) *Scaling analysis and prediction of thermal aspects of the plasma spraying process using a discrete particle approach.* J. Thermal Spray Tech., **11**, 179 - 185

[77] Lee, M.M., Hanratty, T.J. (1988) *The inhibition of droplet deposition by the presence of a liquid wall film.* Int. J. Multiphase Flow, **14**, 129 - 140

[78] Lee, T., Lin, C.-L. (2005) *A stable discretization of the lattice Boltzmann equation for simulation of incompressible two-phase flows at high density ratio.* J. Comp. Physics, **206**, 16 - 47

[79] Lee, S.H., Ryou, H.S. (2000) *Modeling of spray-wall interactions considering liquid film formation.* Proc. 6^{th} Int. Conf. Liquid Atom. Spray Systems, Pasadena, USA

[80] Lenard, P. (1915) *Über Wasserfallelektrizität und über die Oberflächenbeschaffenheit der Flüssigkeiten.* Ann. Physics, **47**, 463 - 524

[81] Leneweit, G., Koehler, R., Roesner, K.G., Schäfer, G. (2005) *Regimes of drop morphology in oblique impact on deep fluids.* J. Fluid Mech., **543**, 303 - 331

[82] Lesser, M.B. (1981) *Analytic solutions of liquid-drop impact droplets.* Proc. R. Soc. London - A, **377**, 289 - 308

[83] Levin, Z., Hobbs, P.V. (1971) *Splashing of water drops on solid and wetted surfaces: hydrodynamics and charge separation.* Proc. R. Soc. London - A, **269**, 555 - 585

[84] Lin, D., Angarita-Jaimes, N.C., Chen, S., Greenaway, A.H., Towers, C.E., Towers, D.P. (2008) *Three-dimensional particle imaging by defocusing method with an annular aperture.* Optics Letters, **33**, 905 - 907

[85] Lindken, R., Di Silvestro, F., Westerweel, J., Nieuwstadt, F. (2002) *Turbulence measurements with μ-PIV in large-scale pipe flow.* Proc. 11^{th} Int. Symp. Appl. Laser Tech. Fluid Mech., Lisbon, Portugal

[86] Lindken, R., Westerweel, J., Wieneke, B. (2006) *Stereoscopic micro particle image velocimetry.* Exp. Fluids, **41**, 161 - 171

[87] Liow, J.L. (2001) *Splash formation by spherical drops.* J. Fluid Mech., **427**, 73 - 105

[88] Longuet-Higgins, M.S. (1990) *An analytic model of sound producing by raindrops.* J. Fluid Mech., **214**, 395 - 410

[89] Macklin, W.C., Hobbs, P.V. (1969) *Subsurface phenomena and the splashing of drops on shallow liquids.* Science, **166**, 107 - 108

[90] Malkiel, E., Sheng, J., Katz, J., Strickler, J.R. (2003) *The three-dimensional flow field generated by a feeding calanoid copepod measured using digital holography.* J. Exp. Biology, **206**, 3657 - 3666

[91] Matsumoto, S., Saito, S. (1970) *On the mechanism of suspension of particles in horizontal conveying: Monte Carlo simulation based on the irregular bouncing model.* J. Chem. Eng. Japan, **3**, 83 - 92

[92] Matsushita, H. (1993) *Color separation/synthetic optical system including two dichroic mirrors angled for correction of astigmatism.* Internet: http://www.freepatentsonline.com/5200857.html

[93] Meingast, U., Staudt, M., Reichelt, L., Renz, U., Sommerhoff, F.A. (2000) *Analysis of spray/wall interaction under diesel engine conditions.* SAE 2000-01-0272

[94] Meinhart, C.D., Barnhart, D.H., Adrian, R.J. (1994) *An interrogation and vector validation system for holographic particle image fields.* Proc. 7^{th} Int. Symp. Appl. Laser Tech. Fluid Mech., Lisbon, Portugal

[95] Meinhart, C.D., Wereley, S.T., Santiago, J.G. (1999) *PIV measurements of a microchannel flow.* Exp. Fluids, **27**, 414 - 419

[96] Meinhart, C.D., Wereley, S.T., Santiago, J.G. (2000) *Micron resolution velocimetry techniques.* Proc. 9^{th} Int. Symp. Appl. Laser Tech. Fluid Mech., Lisbon, Portugal

[97] CVI Mcllcs Griot *Corrccting astigmatism in diodc lascrs.* Intcrnct: http://www.mellesgriot.com/pdf/corast.pdf

[98] Mahammadi, A., Miwa, K., Kidoguchi, Y. (2000) *High time-space resolution analysis of droplets behaviour and gas entrainment into diesel sprays impinging on a wall.* Proc. 16^{th} Ann. Conf. Liquid Atom. Spray Systems, Darmstadt, Germany

[99] Monnier, J.C. (1999) *3D correlation analysis applied to HPIV images*. EUROPIV report no. 34PT05

[100] Morton, D., Rudman, M., Jong-Leng, L. (2000) *An investigation of the flow regimes resulting from splashing drops*. Phys. Fluids, **12**, 747 - 763

[101] Mudawar, I. (2000) *Assessment of high-heat-flux thermal management schemes*. Proc. 7^{th} Intersociety Conf. Thermal and Thermomechanical Phenomena in Electronic Systems, Las Vegas, USA

[102] Mundo, C., Sommerfeld, M., Tropea, C. (1995) *Droplet-wall collisions: experimental studies of the deformation and breakup process*. Int. J. Multiphase Flow, **21**, 151 - 173

[103] Mundo, C., Sommerfeld, M., Tropea, C. (1998) *On the modeling of liquid sprays impinging on surfaces*. Atom. Sprays, **8**, 625 - 652

[104] Nagaoka, M., Kawazoe, H., Nomura, N. (1994) *Modeling fuel spray impingement on a hot wall for gasoline engines*. SAE 940525

[105] Nedderman, R.M. (1961) *The use of stereoscopic photography for the measurement of velocities in liquids*. Chem. Eng. Sci., **16**, 113 - 119

[106] O$\tilde{g}$uz, H.N., Prosperetti, A. (1990) *Bubble entrainment by the impact of drops on liquid surfaces*. J. Fluid Mech., textbf219, 143 - 179

[107] Okawa, T., Shiraishi, T., Mori, T. (2008) *Effect of impingement angle on the outcome of single water drop impact onto a plane water surface*. Exp. Fluids, **44**, 331 - 339

[108] OpenCFD Ltd. (2007) Internet: http://www.opencfd.co.uk/

[109] O'Rourke, P.J. (1981) *Collective drop effects on vaporizing liquid sprays*. Ph.D. Thesis, Princeton University, USA

[110] O'Rourke, P.J., Amsden, A.A. (1996) *A particle numerical model for wall film dynamics in port-injected engines*. SAE 961961

[111] O'Rourke, P.J., Amsden, A.A. (2000) *A spray/wall interaction submodel for the KIVA-3 wall film model*. SAE 2000-01-0271

[112] Özdemir, I.B (1992) *Correlation between the size characteristics of the wall jet and the dynamics of the unsteady film formed after the impingement of an unsteady two-phase jet*. Proc. 6^{th} Int. Symp. Appl. Laser Tech. Fluid Mech., Lisbon, Portugal

[113] Park, K. (1994) *Development of a non-orthogonal-grid computer code for the optimization of direct-injection diesel engine combustion chamber shapes*. Ph.D. Thesis, University of Manchester Institute of Science and Technology, UK

[114] Park, S.W., Lee, C.S. (2004) *Macroscopic and microscopic characteristics of a fuel spray*. Exp. Fluids, **37**, 745 - 762

[115] Pautsch, A.G., Shedd, T.A. (2005) *Spray impingement colling with single- and multiple-nozzle arrays. Part I: Heat transfer data using FC-72*. Int. J. Heat Mass Transfer, **48**, 3167 - 3175

[116] Pautsch, A.G., Shedd, T.A. (2006) *Adiabatic and diabatic measurements of the liquid film thickness during spray cooling with FC-72.* Int. J. Heat Mass Transfer, **49**, 2610 - 2618

[117] Pereira, F., Gharib, M., Dabiri, D., Modarress, D. (2000) *Defocusing digital particle image velocimetry: a 3-component 3-dimensional DPIV measurement technique. Application to bubbly flows.* Exp. Fluids, **Suppl**, S78 - S84

[118] Pereira, F., Gharib, M. (2002) *Defocusing digital particle image velocimetry and the three-dimensional characterization of two-phase flows.* Meas. Sci. Technol., **13**, 683 - 694

[119] Prasad, A.K., Adrian, R.J. (1993) *Stereoscopic particle image velocimetry applied to liquid flows.* Exp. Fluids, **15**, 49 - 60

[120] Prosperetti, A., Oğuz, H.N. (1993) *The impact of drops on liquid surfaces and the underwater noise of rain.* Ann. Rev. Fluid Mech., **25**, 577 - 602

[121] Pumphrey, H.C., Elmore, P.A. (1990) *The entrainment of bubbles by drop impacts.* J. Fluid Mech., **220**, 539 - 567

[122] Qian, J., Law, C.K. (1997) *Regimes of coalescence and separation in droplet collision.* J. Fluid Mech., **331**, 59 - 80

[123] Racca, R.G., Dewey, J.M. (1988) *A method for automatic particle tracking in a three-dimensional flow fluid.* Exp. Fluids, **6**, 25 - 32

[124] Raffel, M., Willert, C.E., Wereley, S., Kompenhans, J. (1998) *Particle image velocimetry: A practical guide.* Springer Verlag, Berlin Heidelberg New York, 1998

[125] Range, K., Feuillebois, F. (1998) *Influence of surface roughness on liquid drop impact.* J. Colloid Interface Sci., **203**, 16 - 30

[126] Rein, M. (1993) *Phenomena of liquid drop impact on solid and liquid surface.* Fluid Dyn. Res., **12**, 61 - 93

[127] Rein, M. (1996) *The transitional regime between coalescing and splashing drops.* J. Fluid Mech., **306**, 145 - 165

[128] Richter, B., Dullenkopf, K., Bauer, H.-J. (2004) *Untersuchung der Eigenschaften von Sekundärtropfen beim Tropfenaufprall auf heiße Wände.* Lasermethoden in der Strömungsmesstechnik, Karlsruhe, Germany

[129] Rieber, M., Frohn, A. (1999) *A numerical study on the mechanism of splashing.* Int. J. Heat Fluid Flow, **20**, 455 - 461

[130] Rioboo, R., Marengo, M., Tropea, C. (2001) *Outcomes from a drop impact on solid surfaces.* Atom. Sprays, **11**, 155 - 165

[131] Rioboo, R., Bauthier, C., Conti, J., Vou'c, M., Dc Coninck, J. (2003) *Experimental investigation of splash and crown formation during single drop impact on wetted surfaces.* Exp. Fluids, **35**, 648 - 652

[132] Rodriguez, F., Mesler, A. (1988), *The penetration of drop-formed vortex rings into pools of liquid.* J. Colloid Interface Sci., **121**, 121 - 129

[133] Roisman, I.V., Araneo, L., Marengo, M., Tropea, C. (1999) *Evaluation of drop impingement models: experimental and numerical anlysis of a spray impact.* Proc. 15^{th} Ann. Conf. Liquid Atom. Spray Systems, Toulouse, France

[134] Roisman, I.V., Tropea, C. (2000) *Flux measurements in sprays using phase doppler techniques.* Atom. Sprays, **11**, 673 - 705

[135] Roisman, I.V., Tropea, C. (2002) *Flow on a wall surface due to spray impact.* Proc. 18^{th} Ann. Conf. Liquid Atom. Spray Systems, Zaragoza, Spain

[136] Roisman, I.V., Rioboo, R., Tropea, C. (2002) *Normal impact of a liquid drop on a dry surface: model for spreading and receding.* Proc. R. Soc. London - A, **458**, 1411 - 1430

[137] Roisman, I.V., Tropea, C. (2002) *Impact of a drop onto a wetted wall: description of crown formation and propagation.* J. Fluid Mech., **472**, 373 - 397

[138] Roisman, I.V., Tropea, C. (2005) *Fluctuating flow and jetting in a liquid layer created by an impacting spray.* Int. J. Multiphase Flow, **31**, 179 - 200

[139] Roisman, I.V., Tropea, C. (2005) *Fluctuating flow in a liquid layer and secondary spray created by an impacting spray.* Int. J. Multiphase Flow, **31**, 179 - 200

[140] Royer, H. (1998) *Three component HPIV with a single angle of view.* EUROPIV report no. 17PT10

[141] Ruck, B. (Ed.) (1990) *Lasermethoden in der Strömungsmesstechnik.* AT-Fachverlag, Stuttgart, 1990

[142] Saito, A., Kawamura, K., Watanabe, S., Takahashi, T., Tuzuki, N. (1993) *Analysis of impinging spray characteristics under high-pressure fuel injection (1st report, measurements of impinging spray characteristics).* Trans. Jap. Soc. Mech. Eng. Part B, **59**, 3290 - 3295

[143] Saito, A., Kawamura, K. (1997) *Behavior of fuel film on a wall at fuel spray impinging.* Proc. 13^{th} Int. Conf. Liquid Atom. Spray Systems, Seoul, Japan

[144] Samenfink, W. (1997) *Grundlegende Untersuchung zur Tropfeninteraktion mit schubspannungsgetriebenen Wandfilmen.* Ph.D. Thesis, Universität Karlsruhe, Germany

[145] Santiago, J.G., Wereley, S.T., Meinhart, C.D., Beebe, D.J., Adrian, R.J. (1998) *A particle image velocimetry system for microfluidics.* Exp. Fluids, **25**, 316 - 319

[146] Scarano, F. 2002 *Iterative image deformation methods in PIV.* Meas. Sci. Technol., **13**, R1 - R19

[147] Schotland, R.M. (1960) *Experimental results relating to the coalescence of water drops with water surfaces.* Discuss. Faraday Soc., **30**, 72 - 77

[148] Schünemann, E., Fedrow, S., Leipertz, A. (1998) *Droplet size and velocity measurements for the characterization of a DI-diesel spray impinging on a flat wall.* SAE 982545

[149] Schäfer, M. (1999) *Numerik im Maschinenbau.* Springer-Verlag Berlin Heidelberg New York, 1999

[150] Shedd, T.A., Pautsch, A.G. (2005) *Spray impingement colling with single- and multiple-nozzle arrays. Part II: Visualisation and emperical models.* Int. J. Heat Mass Transfer, **48**, 3176 - 3184

[151] Sheng, J., Malkiel, E., Katz, J. (2003) *Single beam two-views holographic particle image velocimetry.* Appl. Opt., **42**, 235 - 250

[152] Schimpf, A., Kallweit, S., Richon, J.B. (2003) *Photogrammetric particle image velocimetry.* Proc. 5^{th} Int. Symp. Particle image Velocimetry, Busan, Korea

[153] Shin, J., McMahon, T.A. (1990) *The tuning of a splash.* Phys. Fluids - A, **2**, 1312 - 1317

[154] Shinohara, K., Sugii, Y., Jeong, J.H., Okamoto, K. (2005) *Development of 3D scanning micro-PIV system.* Proc. 6^{th} Int. Symp. Particle image Velocimetry, Pasadena, USA

[155] Sinha, S.K., Kuhlman, P.S. (1992) *Investigating the use of stereoscopic particle streak velocimetry for estimating the three-dimensional vorticity field.* Exp. Fluids, **12**, 337 - 384

[156] Sivakumar, D., Tropea, C. (2002) *Splashing impact of a spray onto a liquid film.* Phys. Fluids, **14**, L85 - L88

[157] Siwon, B., Ennaoui, M., (1991) *Calculating hydrodynamics problems for a liquid film flowing radially on a flat horizontal surface.* Int. J. Num. Methods Fluids, **13**, 655 - 666

[158] Smith, W. (1966) *Modern optical engineering.* McGraw-Hill, 1966

[159] Soria, J., Atkinson, C. (2008) *Towards 3C-3D digital holographic fluid velocity vector field measurement - tomographic digital holographic PIV (Tomo-HPIV).* Meas. Sci. Technol., **19**, 1 - 12

[160] Spurk, J.H. (1987) *Strömungslehre. Eine Einführung in die Theorie der Strömungen.* Springer Verlag, Berlin Heidelberg New York, 1987

[161] Stanton, D.W., Rutland, C. (1996) *Modeling fuel film formation and wall interaction in Diesel Engines.* SAE 960628

[162] Stow, C.D., Stainer, R.D. (1977), *The physical products of a splashing water drop.* J. Meteorol. Soc. Japan, **55**, 518 - 531

[163] Stow, C.D., Hadfield, M.G. (1981), *An experimental investigation of fluid flow resulting from the impact of a water drop with an unyielding dry surface.* Proc. R. Soc. London - A, **373**, 419 - 441

[164] Tao, B., Katz, J., Meneveau, C. (2002) *Statistical geometry of subgrid-scale stresses determined from holographic particle image velocimetry measurements.* J. Fluid Mech., **457**, 35 - 78

[165] Thoroddsen, S.T., Etoh, T.G., Takehara, K. (2003) *Air entrapment under an impacting drop.* J. Fluid Mech., **478**, 125 - 134

[166] Tilton, D.E., Charles, C.L., Pais, M.R., Morgan, M.J. (1992) *High-flux spray cooling in a simulated chip module.* HTD., **206-2**, 73 - 79

[167] Tomonaga, T., Murai, K., Takano, T., Sami, H. (1996) *A study on the combustionbehavior of a diesel fuel spray impinging on a wall.* SAE 960028

[168] Torres, J.H., Nelson, J.S., Tanenbaum, B.S., Milner, T.E., Goodman, D.M., Anvari, B. (1999) *Estimation of internal skin temperature in response to cryogen spray cooling: implications for laser therapy of port wine stains.* IEEE Journal of Selected Topics in Quantum Electronics, **4**, 1058 - 1066

[169] Towers, C.E., Towers, D.P., Campbell, H.I., Zhang, S., Greenaway, A.H. (2006) *Three-dimensional particle imaging by wavefront sensing.* Optics Letters, **31**, 1220 - 1222

[170] Tropea, C., Marengo, M. (1998) *The impact of drops on walls and films.* Proc. 3^{th} Int. Conf. Multiphase Flow, Lyon, France

[171] Tropea, C., Roisman, I.V. (2000) *Modeling of spray impact on solid surfaces.* Atom. Sprays, **10**, 387 - 408

[172] Trujillo, M.F., Mathews, W., Lee, C.F., Peters, J.E. (1998) *A computational and experimental investigation of spray/wall impingement.* Proc. 11^{th} Ann. Conf. Liquid Atom. Spray Systems - Americas, Sacramento, USA

[173] Trujillo, M.F., Lee, C.F. (2001) *Modeling crown formation due to the splashing of a droplet.* Phys. Fluids, **13**, 2503 - 2516

[174] Trujillo, M.F., Lee, C.F. (2003) *Modeling Film dynamics in spray impingement.* J. Fluid Eng., **125**, 104 - 112

[175] Udrea, D.D., Bryanston-cross, P.J., Moroni, M., Querzoli, G. (2000) *Particle tracking velocimetry techniques.* Particle Image Velocimetry: Progress towards Industrial Application, Kluwer Academic Publishers, 2000

[176] Vander Wal, R.L., Berger, G.M., Mozes, S.D. (2006) *The splash/non-splash boundary upon a dry surface and thin fluid film.* Exp. Fluids, **40**, 53 - 59

[177] Veerman, H.P.J., Den Boer, R.J.W. (2000) *PIV measurements in presence of a large out of plane component.* Particle Image Velocimetry: Progress towards Industrial Application, Kluwer Academic Publishers, 2000

[178] Virant, M., Dracos, T. (1996) *Establishment of a videogrammetric PTV system.* Three-dimensional velocity and vorticity measureing and image analysis techniques, Kluwer Academic Publishers, 1996

[179] Virant, M. (1996) *Anwendung des dreidimensionalen 'particle tracking-velocimetry' auf die Untersuchung von Dispersionsvorgängen in Kanalströmungen.* Ph.D. thesis, ETH Zürich, Switserland

[180] Wachters, L.H.J., Westerling, N.A.J. (1966) *The heat transfer from a hot wall to impinging water drops in a spherical state.* Chem. Eng. Science, **21**, 1047 - 1056

[181] Walzel, P. (1980) *Zeteilgrenze beim Tropfenaufprall.* Chem.-Ing.-Tech., **52**, 338 - 339

[182] Wang, A.B., Chen, C.C. (2000) *Splashing impact of a single drop onto very thin liquid films.* Phys. Fluids, **12**, 2155 - 2158

[183] Wang, M., Watkins, A.P. (1993) *Numerical modelling of diesel spray impaction phenomena*. Int. J. Heat Fluid Flow, **14**, 310 - 311

[184] Watkins, A.P., Wang, D.M. (1990) *A new model for diesel spray impaction on walls and comparison with experiments*. Int. Symp. Diagnostics and Modelling Combustion I.C. Engines, Kyoto, Japan

[185] Weiss, C., Yarin, A.L. (1999) *Single drop impact onto liquid films: neck distortion, jetting, tiny bubble entrainment, and crown formation*. J. Fluid Mech., **385**, 229 - 254

[186] Weiss, C. (2005) *The liquid deposition fraction of sprays impinging vertical walls and flowing films*. Int. J. Multiphase Flow, **31**, 115 - 140

[187] Wenzel, S. (2001) *Ausbreitung von Kraftstoffsspray beim Aufprall auf eine feste Oberfläche: Einflußvon Wandgeometry und Umgebungsdruck*. Master thesis, Technische Universität Darmstadt, Germany

[188] Westerweel, J., Nieuwstadt, F.T.M. (1991) *Performance tests on 3-dimensional velocity measurements with a two-camera digital particle image velocimeter*. ASME Laser Anemometry, **1**, 349 - 355

[189] Westerweel, J. (1994) *Efficient detection of spurious vectors in particle image velocimetry data*. Exp. Fluids, **16**, 236 - 247

[190] Westerweel, J., van Oord, J. (2000) *Stereoscopic PIV measurements in a turbulent boundary layer*. Particle Image Velocimetry: Progress towards Industrial Application, Kluwer Academic Publishers, 2000

[191] Wieneke, B. (2005) *Stereo-PIV using self-calibration on particle images*. Exp. Fluids, **39**, 267 - 280

[192] Willert, C.E., Gharib, M. (1991) *Digital particle image velocimetry*. Exp. Fluids, **10**, 181 - 193

[193] Willert, C.E., Gharib, M. (1992) *Three-dimensional particle imaging with a single camera*. Exp. Fluids, **12**, 353 - 358

[194] Wu, Z.N. (1992) *Modélisation et calcul implicite multidomaine d'écoulements diphasiques gaz-gouttelettes*. Ph.D. Thesis, Université Pierre et Marie Curie, France

[195] Yarin, A.L., Rubin, M.B., Roisman, I.V. (1995) *Penetration of a rigid projectile into an elastic-plastic target of finite thickness*. Int. J. Impact Eng., **16**, 801 - 831

[196] Yarin, A.L., Weiss, D.A. (1995) *Impact of drops on solid surfaces: self-similar capillary waves, and splashing as a new type of kinematic discontinuity*. J. Fluid Mech., **283**, 141 - 173

[197] Yasuda, K., Ninomiya, N., Sugiyama, H., Hitomi, D. (2005) *Simultancous PIV mcasurcment of the flow around and inside a falling drop*. Proc. 6^{th} Int. Symp. Particle image Velocimetry, Pasadena, USA

[198] Ye, Q., Steigleder, T., Scheibe, A., Domnick, J. (2002) *Numerical simulation of the electrostatic powder coating process with a corona spray gun*. J. Electrostat, **54**, 189 - 205

[199] Zhang, J., Tao, B., Katz, J. (1997) *Turbulent flow measurement in a square duct with hybrid holographic PIV*. Exp. Fluids, **23**, 373 - 381

[200] Zhang, F.H., Thoroddsen, S.T. (2008) *Satellite generation during bubble coalescence*. Phys. Fluids, **20**, 1 - 11

[201] Zbhankova, S.L., Kolpakov, A.V. (1990) *Collision of water drops with a plane water surface*. Fluid Dynam., **25**, 470 - 473

Appendix A

Comparison of the experimental data with the analytical model of the cavity diameter at the initial impingement stage

This appendix shows the comparison between the experimentally obtained results of the cavity diameter squared, measured at $y_{cav}/h^* = 0.5$, and the analytical solution given by eq. (4.3) at the initial stage of the cavity expansion.

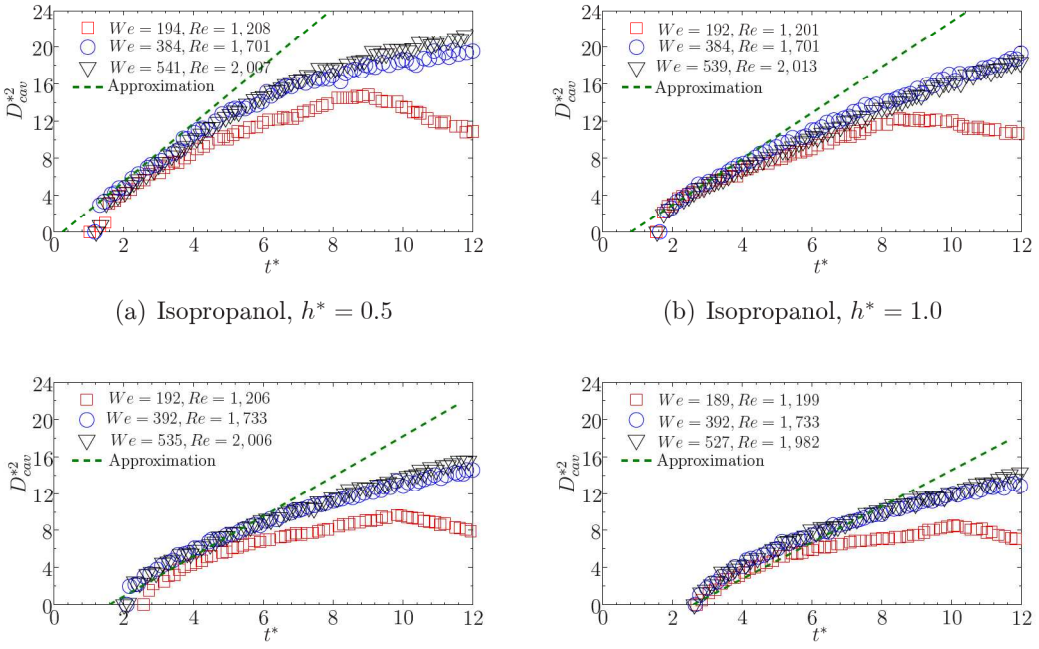

(a) Isopropanol, $h^* = 0.5$

(b) Isopropanol, $h^* = 1.0$

(c) Isopropanol, $h^* = 1.5$

(d) Isopropanol, $h^* = 2.0$

Figure A.1: Comparison of the experimental results with the analytical solution (eq. (4.3)) of the diameters of the cavity for isopropanol at the initial stage of the cavity expansion. The square of the diameter D^*_{cav} is shown as a function of the non-dimensional time t^* for (a) $h^* = 0.5$, (b) $h^* = 1.0$, (c) $h^* = 1.5$ and (d) $h^* = 2.0$. The impingement parameters for the experimental data are listed in Table 4.2

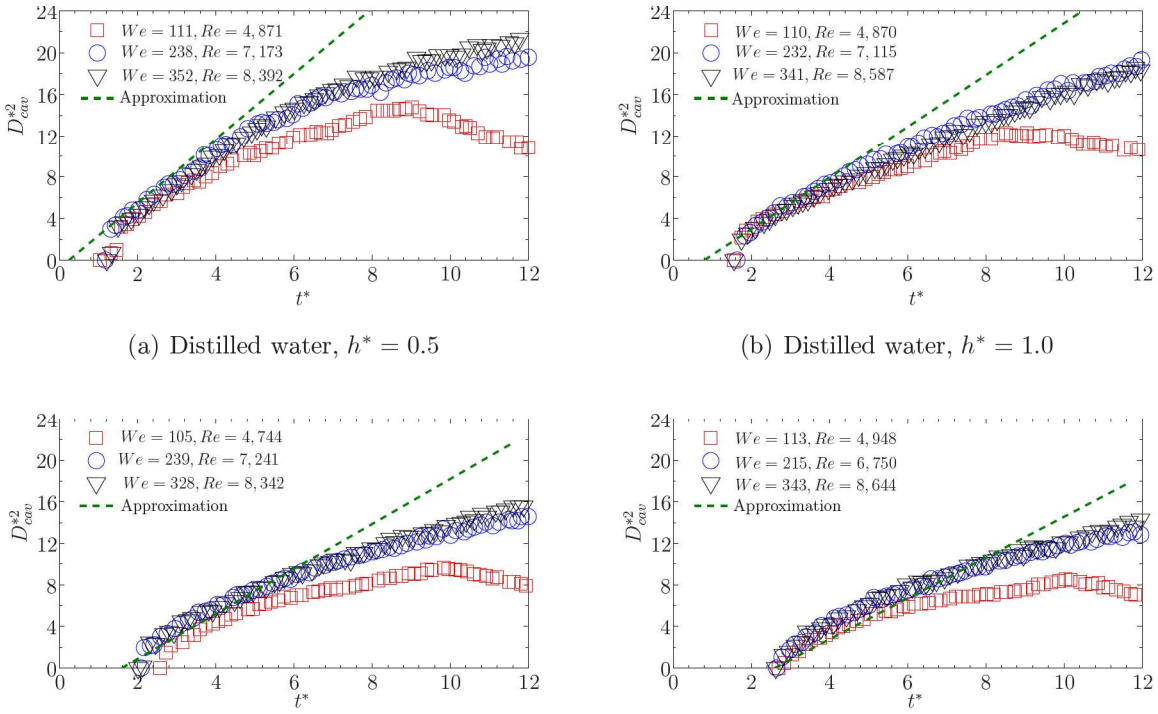

(a) Distilled water, $h^* = 0.5$

(b) Distilled water, $h^* = 1.0$

(c) Distilled water, $h^* = 1.5$

(d) Distilled water, $h^* = 2.0$

Figure A.2: Comparison of the experimental results with the analytical solution (eq. (4.3)) of the diameters of the cavity for distilled water at the initial stage of the cavity expansion. The square of the diameter D^*_{cav} is shown as a function of the non-dimensional time t^* for (a) $h^* = 0.5$, (b) $h^* = 1.0$, (c) $h^* = 1.5$ and (d) $h^* = 2.0$. The impingement parameters for the experimental data are listed in Table 4.2

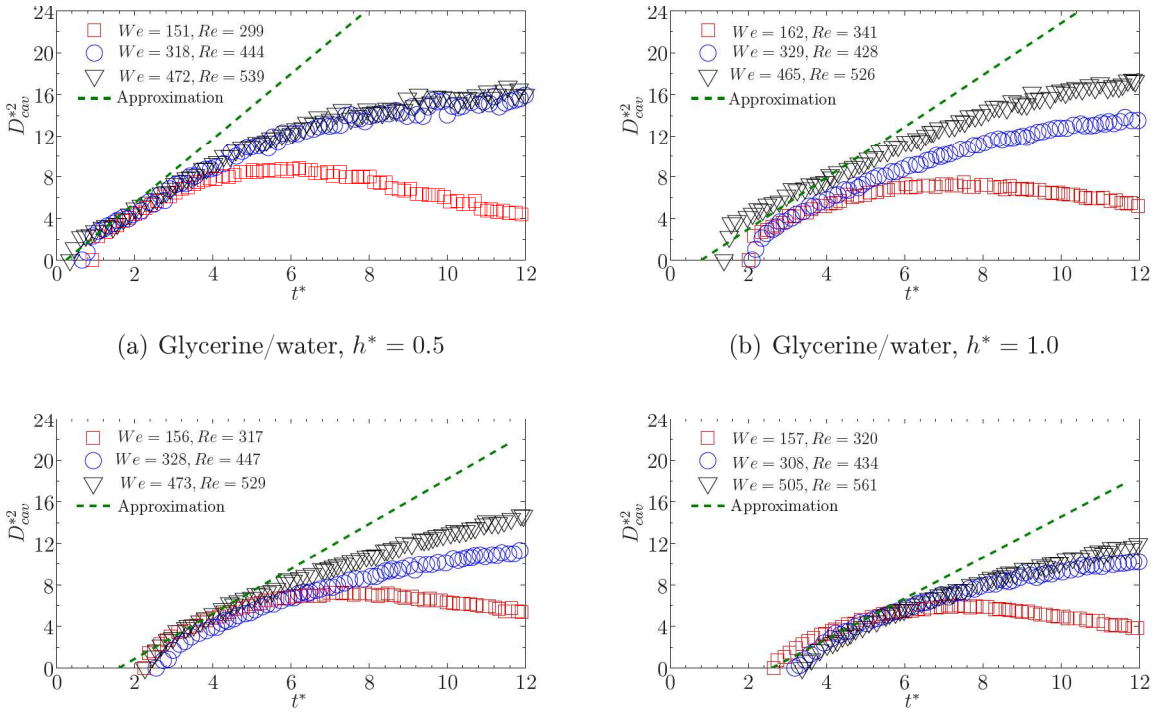

(a) Glycerine/water, $h^* = 0.5$

(b) Glycerine/water, $h^* = 1.0$

(c) Glycerine/water, $h^* = 1.5$

(d) Glycerine/water, $h^* = 2.0$

Figure A.3: Comparison of the experimental results with the analytical solution (eq. (4.3)) of the diameters of the cavity for glycerine/water at the initial stage of the cavity expansion. The square of the diameter D^*_{cav} is shown as a function of the non-dimensional time t^* for (a) $h^* = 0.5$, (b) $h^* = 1.0$, (c) $h^* = 1.5$ and (d) $h^* = 2.0$. The impingement parameters for the experimental data are listed in Table 4.2